TABLE E-I Biomechanical Measurements of Maximum Load, Maximum Stiffness, and Failure Location in Normal Sheep Infraspinatus Tendons Tested in Tension at Different Crosshead Rates*

Crosshead Rate† *(cm/min)*	Maximum Load *(kN)*	Maximum Stiffness *(kN/mm)*	Failure Location *(no. of repairs)*			
			Bone Shaft	Bone Insertion	Tendon	Upper Clamp
2.0 (n = 16)	3.68 ± 0.48[a]	0.289 ± 0.049[a]	13	1	1	1
20.0 (n = 9)	3.76 ± 0.34[a]	0.283 ± 0.059[a]	4	1	3	1
72.0 (n = 9)	3.93 ± 0.74[a]	0.229 ± 0.062[b]	5	2	1	1

*The values are given as the mean and the standard deviation. The values within each column that share the same letter are not significantly different. †The values in this column correspond to 0.5%, 5.5%, and 20% strain/sec, respectively.

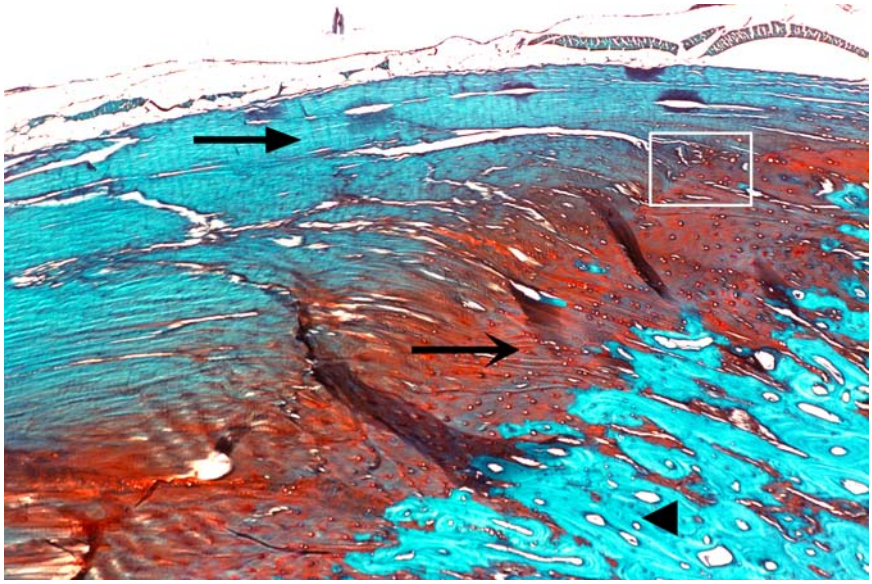

Fig. E1-A

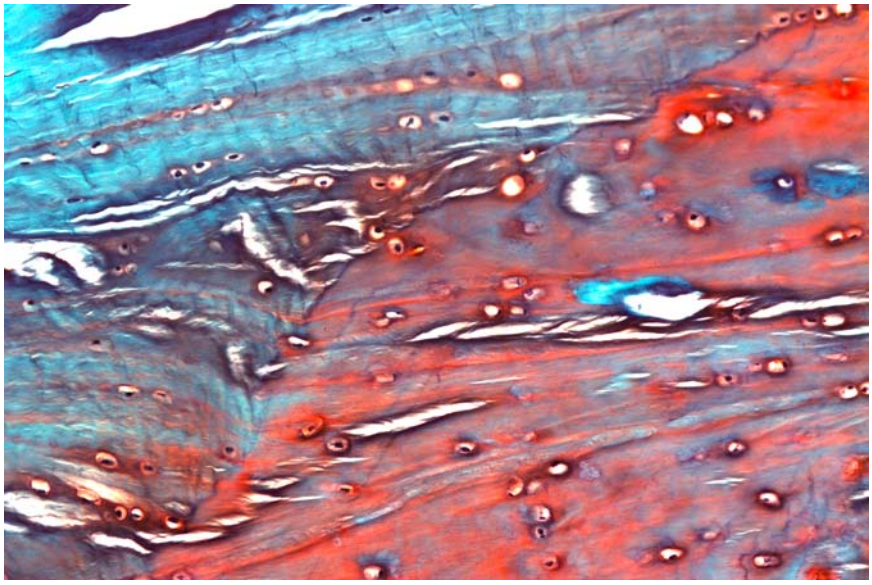

Fig. E1-B

Figs. E1-A and E1-B Histological appearance of the normal infraspinatus tendon (arrow with closed head) and its fibrocartilaginous attachment (arrow with open head) to the proximal part of the humerus (arrowhead). The area within the white box in Fig. E1-A is shown in Fig. E1-B (Weigert safranin-O stain, ×4 for Fig. E1-A and ×20 for Fig. E1-B).

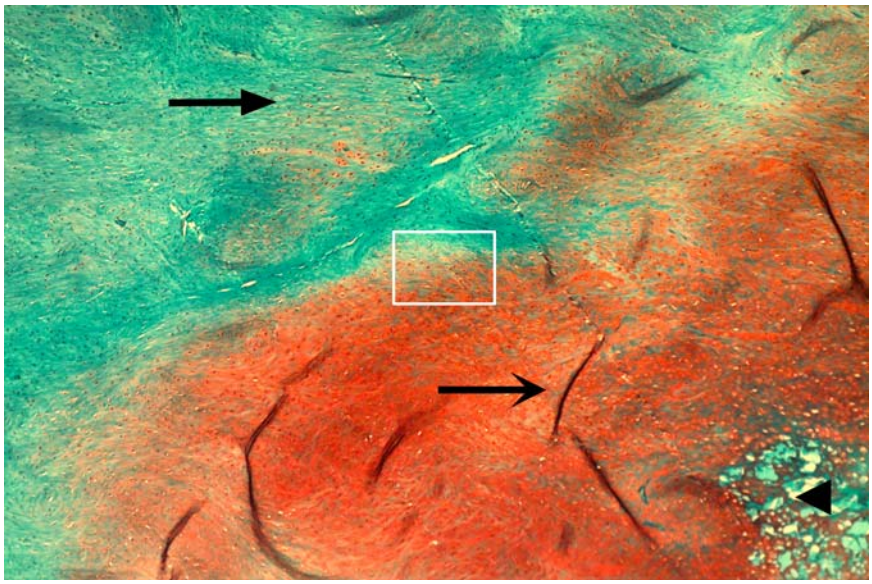

Fig. E1-C

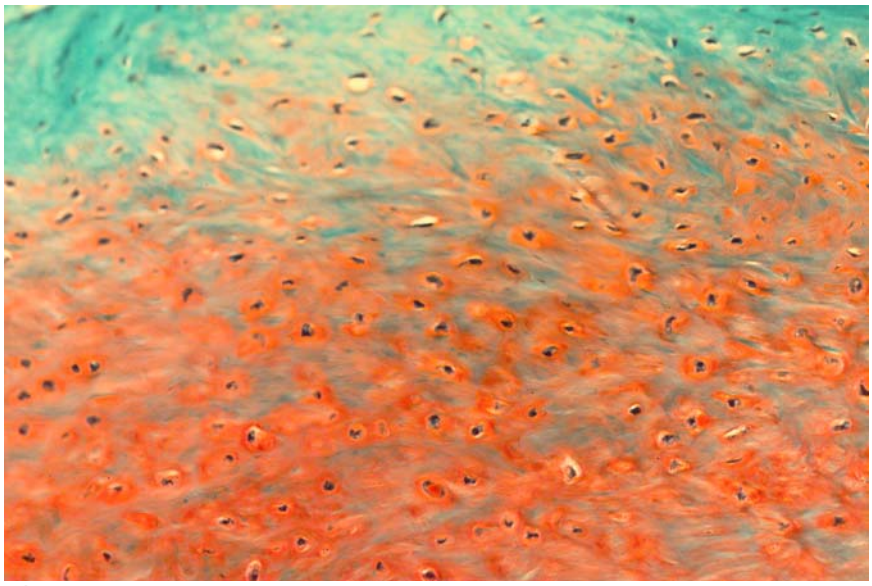

Fig. E1-D

Figs. E1-C and E1-D Corresponding regions in an rhBMP-12/Type-I/III collagen sponge-treated repair. The area within the white box in Fig. E1-C is shown in Fig. E1-D (Weigert safranin-O stain, ×4 for Fig. E1-C and ×20 for Fig. E1-D).

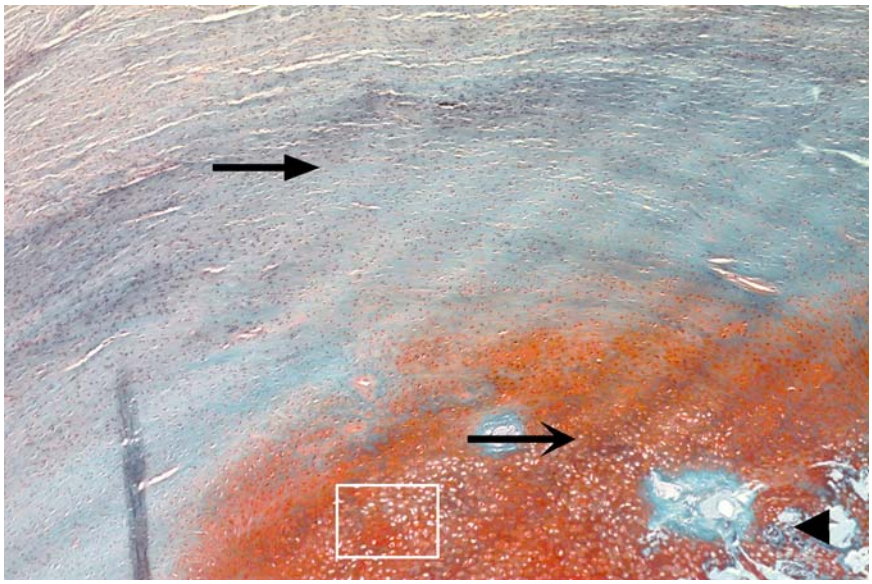

Fig. E1-E

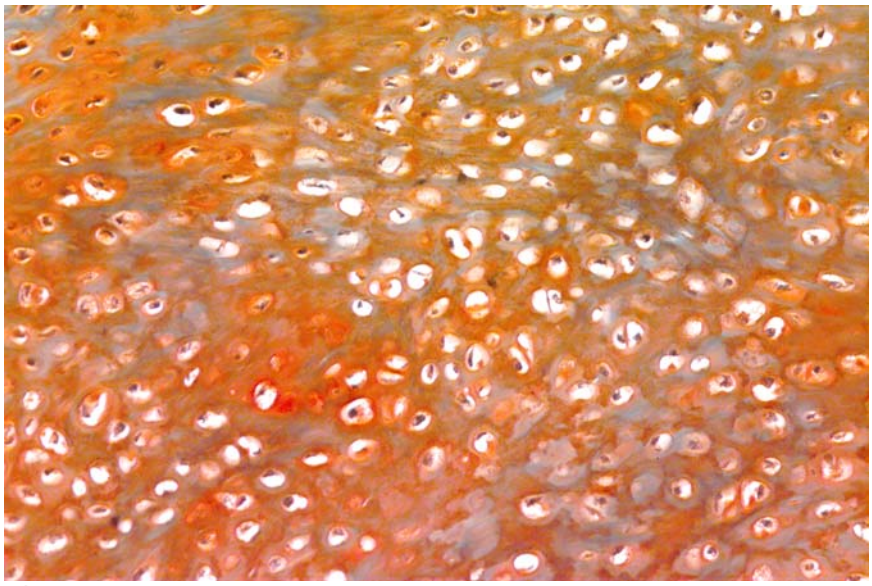

Fig. E1-F

Figs. E1-E and E1-F Corresponding regions in an untreated repair. The area within the white box in Fig. E1-E is shown in Fig. E1-F (Weigert safranin-O stain, ×4 for Fig. E1-E and ×20 for Fig. E1-F).

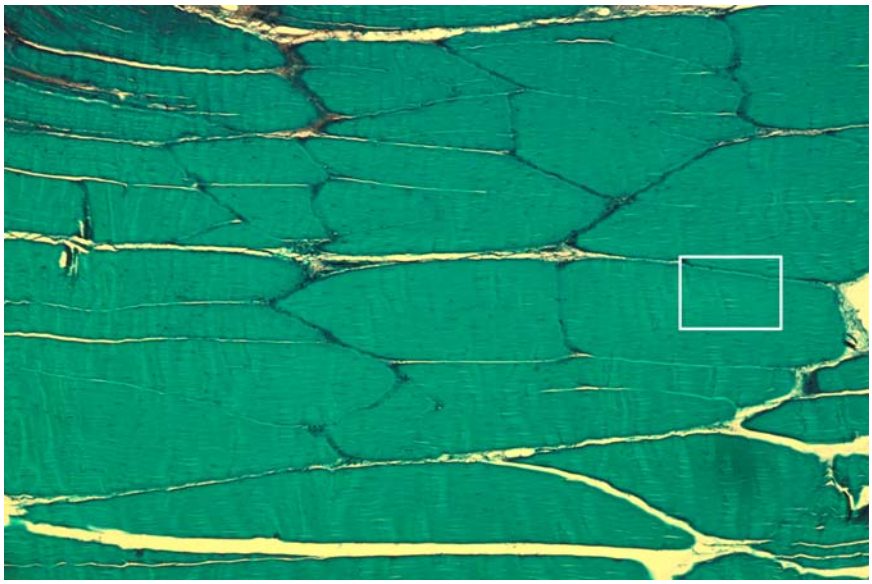

Fig. E2-A

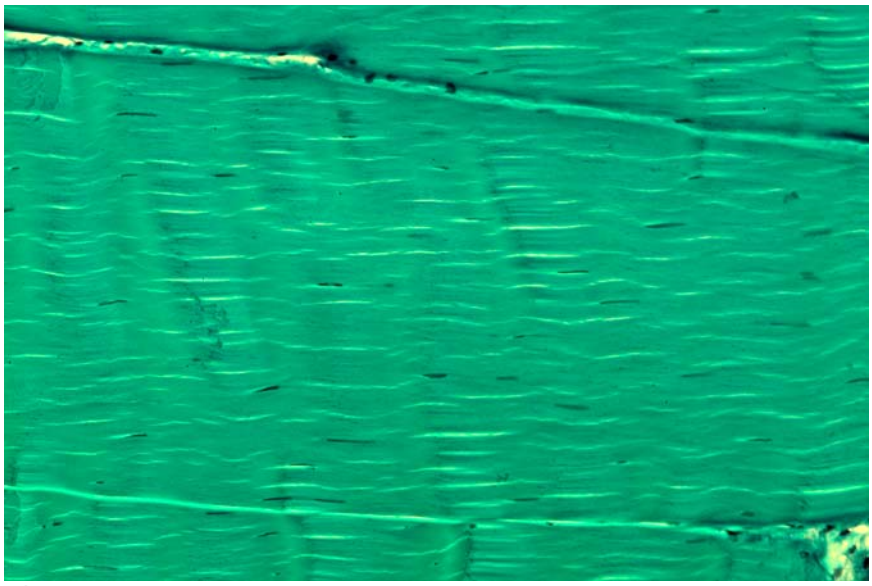

Fig. E2-B

Figs. E2-A and E2-B Histological appearance of the midsubstance of the normal infraspinatus tendon. The area within the white box in Fig. E2-A is shown in Fig. E2-B (Weigert safranin-O stain, ×4 for Fig. E2-A and ×20 for Fig. E2-B).

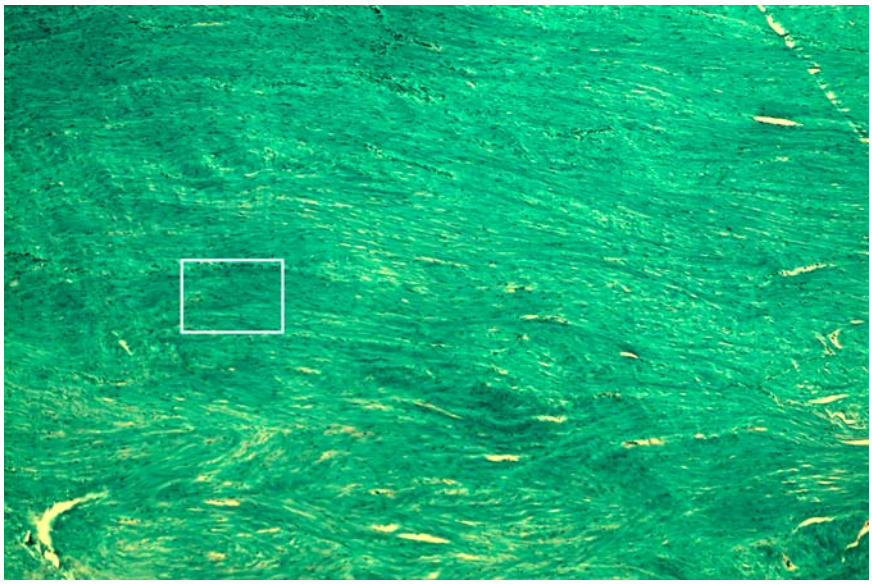

Fig. E2-C

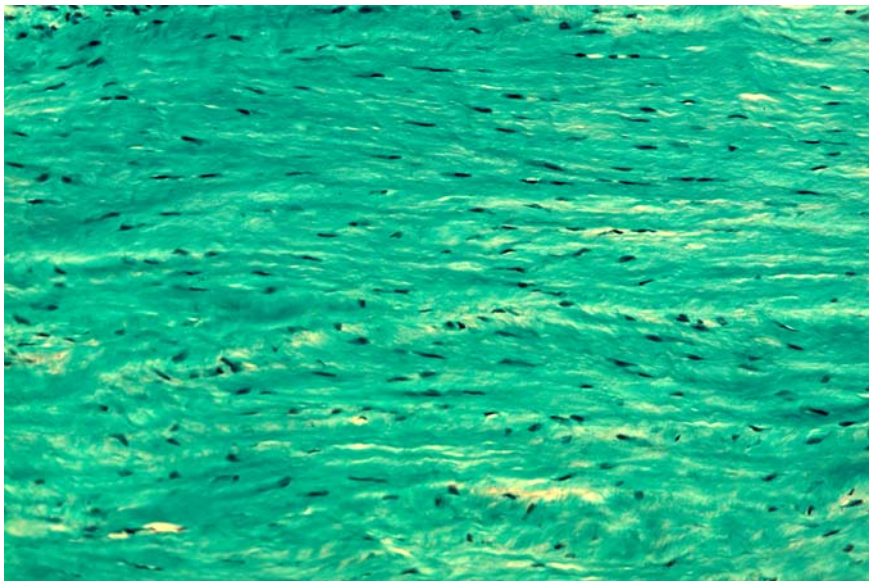

Fig. E2-D

Figs. E2-C and E2-D Histological appearance of the midsubstance of the infraspinatus tendon after an rhBMP-12/Type-I/III collagen sponge-treated repair. The area within the white box in Fig. E2-C is shown in Fig. E2-D (Weigert safranin-O stain, ×4 for Fig. E2-C and ×20 for Fig. E2-D).

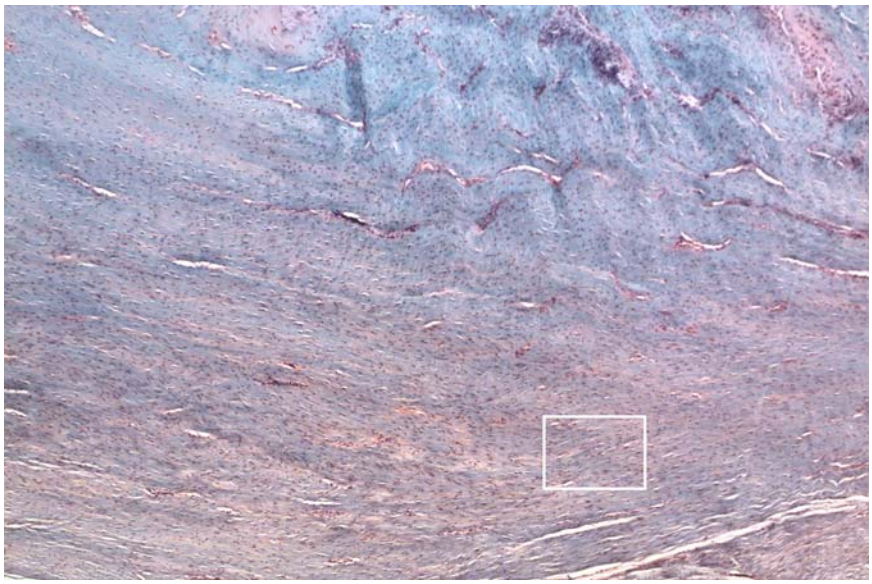

Fig. E2-E

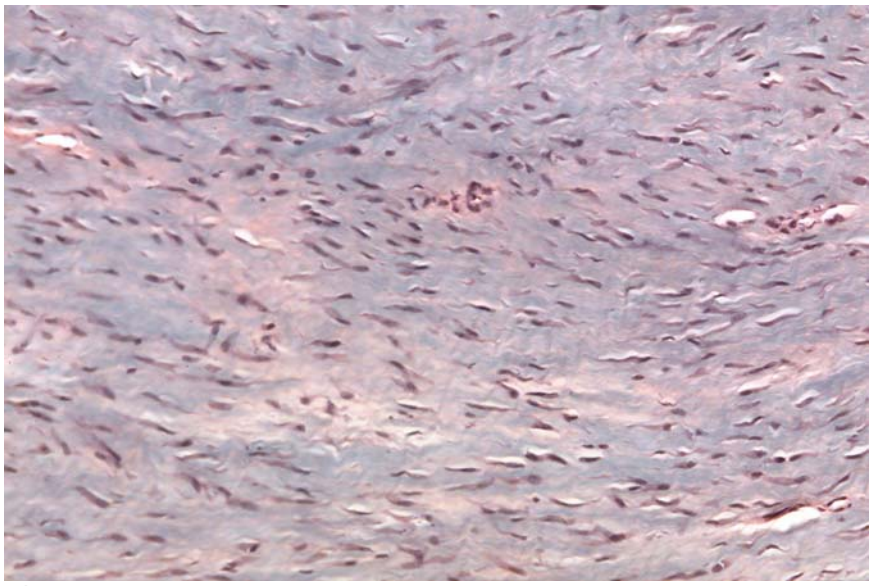

Fig. E2-F

Figs. E2-E and E2-F Histological appearance of the midsubstance of the infraspinatus tendon after an untreated repair. The area within the white box in Fig. E2-E is shown in Fig. E2-F (Weigert safranin-O stain, ×4 for Fig. E2-E and ×20 for Fig. E2-F).

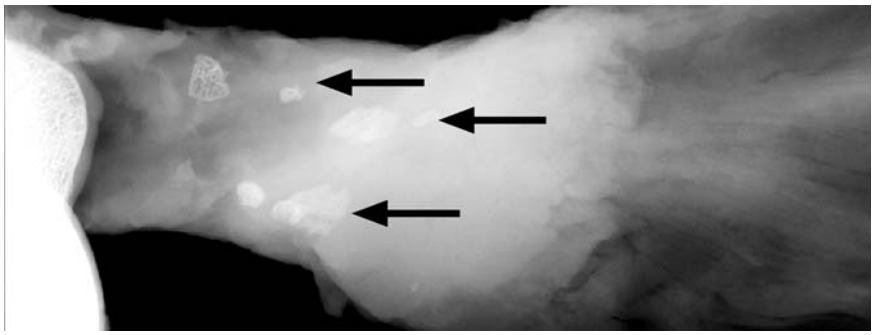

Fig. E3-A

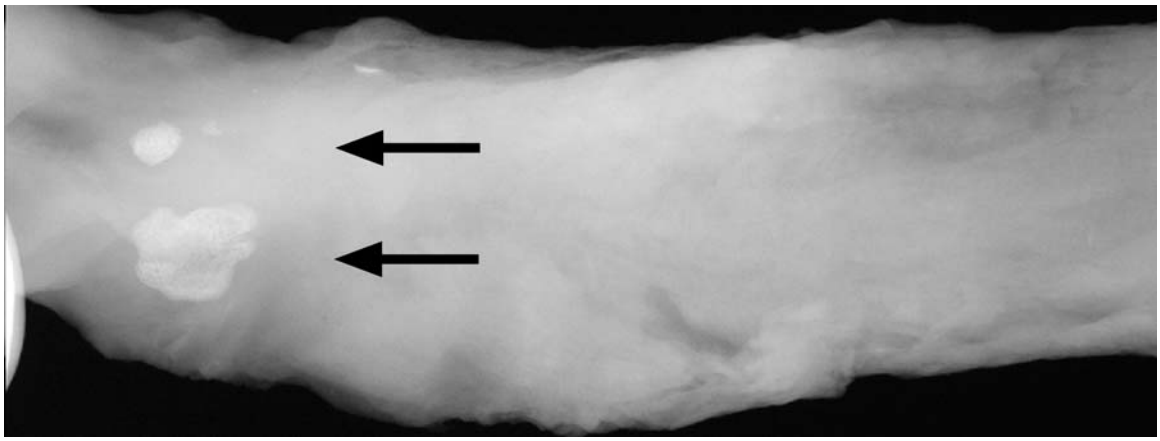

Fig. E3-B

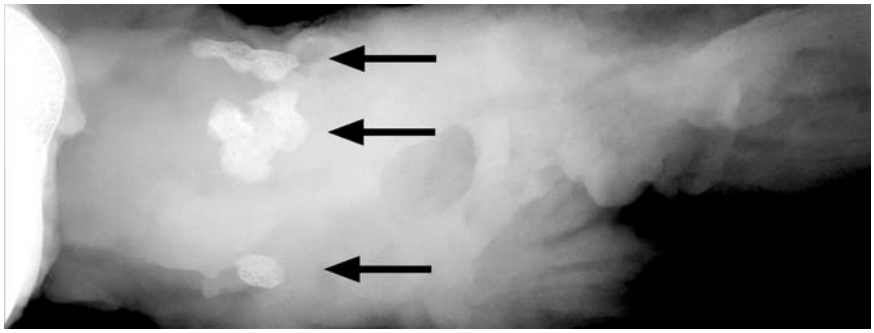

Fig. E3-C

Radiographic appearance of bone nodules (arrows) in an untreated infraspinatus repair (Fig. E3-A) compared with a repair treated with the Type-I/III collagen sponge (Fig. E3-B) and a repair treated with the rhBMP-12 in Type-I/III collagen sponge (Fig. E3-C). The untreated repairs had a higher frequency but smaller size of bone nodules compared with the treated repairs.